Photoionization Cross Section for Manganese Acceptors in Gallium Arsenide*

Winfield J. Brown Jr.,† Dustin A. Woodbury, and J. S. Blakemore
Physics Department, Florida Atlantic University, Boca Raton, Florida 33432
(Received 30 April 1973)

Optical-transmission measurements at 20 and 77 K were used to deduce the magnitude and spectral dependence of the optical cross section σ_I for transitions from neutral Mn acceptors to the valence bands of GaAs. The threshold energy for such transitions is $E_a = 0.11$ eV, and σ_I was studied from threshold to 0.7 eV. The crystals used had 10^{17} to 10^{18} cm^{-3} of uncompensated Mn acceptors, as determined by analysis of Hall-effect data over the 60–400-K range. The spectral dependence of σ_I over the range 0.11–0.45 eV is in good agreement with Lucovsky's δ-function potential model, as has been reported previously. Comparisons between experiment and Lucovsky's model are complicated for photon energies above 0.46 eV by transitions to the split-off band of GaAs. In contrast to previous reports, we find that the magnitude of σ_I (a maximum of 8×10^{-17} cm^2 at 0.22 eV) is in good agreement with Lucovsky's model for an effective-field ratio of unity. Thus we find that dielectric reinforcement of the electric vector for a photon interacting with a Mn acceptor (wave-function radius 10.1 Å) is negligible. A comparison of our data with quantum-defect models is less satisfactory than the δ-function model at low energies, but becomes more favorable in the spectral region for which the split-off band is involved.

I. INTRODUCTION

Elements such as germanium and zinc provide shallow acceptor states in GaAs with a hydrogenic ionization energy $E_H = 0.03$ eV. This behavior is consistent with a Coulomb $(e/\kappa r)$ potential, and suggests a wave-function radius $a_H = (e^2/2\kappa E_H) = 19$ Å. In contrast, transport measurements carried out for Mn-doped GaAs by Vieland, [1] and extended to other transition elements by Haisty and Cronin, [2] show that the acceptors introduced by transition atoms have ionization energies ranging from 0.1 to 0.7 eV. Thus these acceptors are too deep in energy and too small in spatial extent to be appropriate for description in terms of a Coulomb potential. Optical studies of the excited states for Mn by Chapman and Hutchinson[3] show that these are comparable in energy with those of hydrogenic impurities, as is to be expected since the eigenvalues for excited states are influenced primarily by the Coulombic wings of a potential which is much steeper than Coulombic at short range.

Interest in manganese acceptors in GaAs has frequently centered around the luminescent capture of conduction electrons by neutral Mn atoms. [4] However, in this paper we are concerned with transitions between the manganese ground state and the valence bands. Measurements of the threshold energy for extrinsic photoconductance[5] or for photoionization[3,5,6] show that the Mn ground state is at an energy $E_a = 0.11$ eV above the uppermost valence bands. (The thermal activation energy yielded by electrical-transport experiments decreases below 0.11 eV as the density of neutral and/or ionized manganese atoms increases.[7]) As is typical for a deep impurity, the photoionization cross section reaches a maximum for a photon energy of about $2E_a$, and it was apparent from our initial work[5] that the magnitude we deduced for this cross section was considerably smaller than that reported by others.[3,6] More extensive data are now reported, with a discussion of the reported cross sections in the light of deep impurity models.

Within the appropriate spectral range (photon energy larger than E_a but smaller than the intrinsic gap E_i), the photoionization cross section per acceptor, σ_I, is related to the measured optical absorption coefficient α by

$$\alpha = \alpha_r + \sigma_I N_n \ . \tag{1}$$

Here α_r denotes the absorption caused by processes other than photoionization (such as free-carrier absorption, bound-bound excitation, lattice absorption, intraband excitation, etc.). The study of photoionization is simplest if conditions are such that $\alpha_r \ll \alpha$, but this is not always possible. The quantity N_n in Eq. (1) is the density of neutral and ionizable acceptors; for a p-type semiconductor at temperatures low enough to ensure that $p_0 \ll N_d < N_a$, then $N_n = (N_a - N_d)$.

Thus while measurement of α suffices to establish the spectral dependence of σ_I, the magnitude of this cross section cannot be determined without a knowledge of the densities of manganese acceptors (N_a) and compensator centers (N_d). We believe that this lies at the root of the apparent difference between our measurement of σ_I and previous estimates of this quantity,[3,6] for the determination of $N_a - N_d$ in a manganese-doped GaAs containing enough manganese to permit good optical absorption data is not a trivial undertaking. The free-hole density p_0 at room temperature is a poor guide

to $N_a - N_d$, and in three of the four crystals we studied amounted only to some 20% of $N_a - N_d$. We found it necessary to analyze Hall-effect data over a wide temperature range in order to get the most reliable value for $N_a - N_d$ in each crystal, and this information is incorporated into the data quoted in this paper for σ_I.

II. EXPERIMENTAL TECHNIQUES AND RESULTS

Our experimental techniques were straightforward and were based on those described previously,[5] with some improvements. Optical-absorption measurements were made first, with the sample shaped as a plane parallel-sided slab with polished faces. A bridge-shaped sample was subsequently cut from the central portion of this slab for Hall measurements. It is convenient, however, to discuss the material characterization with Hall data first.

Each bridge-shaped Hall sample, with Ohmic, alloyed, In-Zn contacts, was subjected to dc conductivity and Hall measurements. An electrically heated chamber was used from room temperature upwards, while measurements from room temperature downwards were made with the sample mounted in a CryoTip hydrogen-nitrogen Joule-Thomson cooler. Voltages and currents were recorded digitally. A 4000-G magnetic field was used for Hall measurements, which were accordingly made in the "weak-field" regime. Nevertheless, our data were analyzed with the Hall factor r in

$$R_H = r/ep_0 \tag{2}$$

arbitrarily replaced by unity; this will subject our quoted values for $N_a - N_d$ and hence for σ_I to a systematic error which is unlikely to exceed 10%.

Values for $p_0 = 1/eR_H$ at temperatures from 60 to 550 K were fitted to the mass-action equation

$$\frac{p_0(N_d + p_0)}{N_a - N_d - p_0} = \frac{N_v}{\beta} e^{-E_a/kT}$$

$$= 4.27 \times 10^{14} T^{3/2} e^{-E_a/kT} \text{ cm}^{-3} \tag{3}$$

using an IBM 360-44 or a Univac 1108 computer in a nonlinear-least-squares analysis to yield optimized values for the parameters N_a, N_d, and E_a.

TABLE I. Characterization for manganese-doped crystals used.

Crystal	Manganese Conc. N_a(cm^{-3})	Effective compensator density N_d(cm^{-3})	Low-Temp. neutral Mn density $(N_a - N_d)$ (cm^{-3})	Thermal-ionization energy E_a (eV)
*M*1	1.64×10^{17}	4.7×10^{16}	1.17×10^{17}	0.091
*M*5	1.13×10^{18}	5.7×10^{16}	1.07×10^{18}	0.096
*M*6	1.18×10^{18}	2.4×10^{17}	9.43×10^{17}	0.067
*M*7	1.36×10^{18}	2.8×10^{17}	1.07×10^{18}	0.069

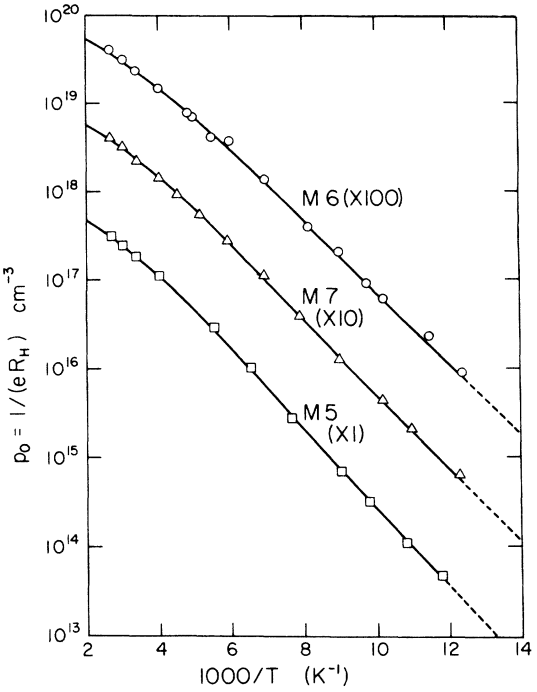

FIG. 1. Free-hole density vs reciprocal temperature for Hall samples from crystals *M*5, *M*6, and *M*7. The curves show computer fits to Eq. (3) for values of the material parameters listed in Table I.

We were able to satisfy ourselves that the restrictions on the range of validity for Eq. (3) were not violated. The material parameter values determined for the four Mn-doped crystals which concern us in this paper are listed in Table I, while computer-generated curves of p_0 vs $(1000/T)$ are superimposed in Fig. 1 on the experimental Hall-effect data points for three of these samples. Figure 1 was drawn at a time when measurements terminated at 400 K, and more recent data points extended to 550 K confirm the analysis.

The predecessor of each Hall-effect sample was the same material as a polished slab of thickness t with plane parallel faces. Optical transmission was measured at 20 or 77 K in a hydrogen-nitrogen CryoTip system equipped with BaF_2 windows; the sample was placed at the second focus of radiation from a Perkin-Elmer 112 monochromator with NaCl optics, and transmitted intensities were measured with a cooled Au-Ge detector. Phase-sensitive detection was used.

The optical transmittance T is the ratio of intensities transmitted by the sample beam and by a similarly collimated reference beam, and we expect T to be related to the optical-absorption coefficient α by

$$T = \frac{(1-R)^2 e^{-\alpha t}}{1 - R^2 e^{-2\alpha t}} \ . \tag{4}$$

Our analog data for T with each sample run was digitized and computer processed to yield a table for "photoabsorption cross section" versus photon energy. This computer program (which also averaged transmissivity data over several runs for a given sample at a given temperature) proceeded upon the assumptions that GaAs has a reflectivity $R = 0.29$, and that the deduced cross section is $[\alpha/(N_a - N_d)]$ under the conditions of optical measurement. Thus this cross section is just σ_I when the quantity α_r in Eq. (1) is negligible, but will exceed σ_I for photon energies or conditions which make α_r significant. Nonetheless, we shall follow normal practice in calling the deduced cross section σ_I in reference to Figs. 2 and 3.

Figure 2 plots σ_I versus photon energy for crystals $M1$, $M5$, $M6$, and $M7$ at 77 K and for $M5$ at 20 K. The figure also reproduces the curves for σ_I reported by Chapman and Hutchinson[3] and by Blätte.[6] A logarithmic ordinate scale is used so that an error in $(N_a - N_d)$ shifts the curve vertically but does not change the shape. As noted in Sec. I, we expect the much larger cross sections deduced by Chapman and Hutchinson[3] and by Blätte[6] to be the consequence of such errors in the evaluation of impurity content. Since these authors were also concerned with the bound-bound excitation line spectrum for Mn centers, their measurements were made at very low temperatures with high resolution; the composite effects of excitation lines account for the apparent extension of a large σ_I to smaller photon energies in the two upper curves of Fig. 2.

The discrete excitation lines of Mn centers were not resolvable in our 77-K data, except for the line identified by Chapman and Hutchinson as the D line shifted upwards by a 0.036-eV LO-phonon energy (i.e., at about 0.14 eV). The resolution was of course improved in the 20-K data for sample $M5$, but the dashed curve in Fig. 2 omits these details in order to concentrate on the broad photoionization band.

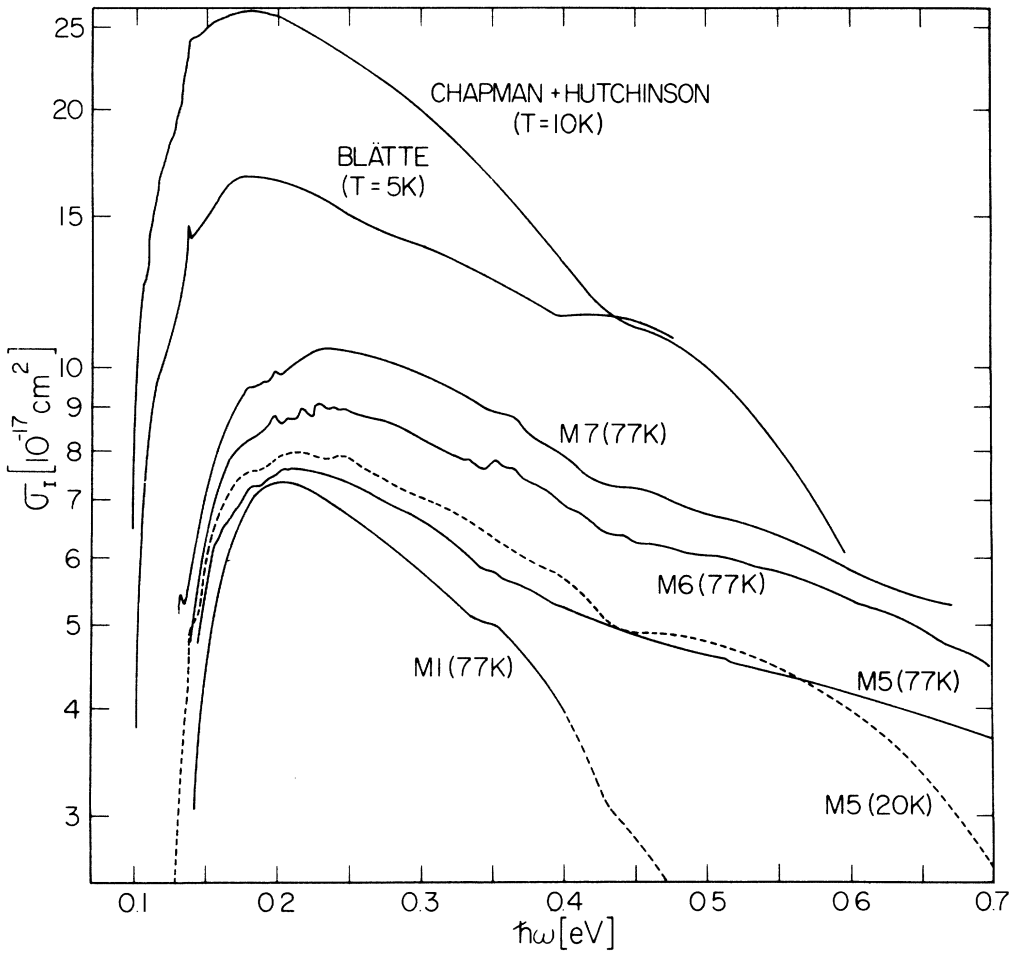

FIG. 2. Photoionization cross section vs photon energy for the four crystals of the present study (crystal $M5$ at both 77 and 20 K), and as reported by Blätte (Ref. 6) and by Chapman and Hutchinson (Ref. 3).

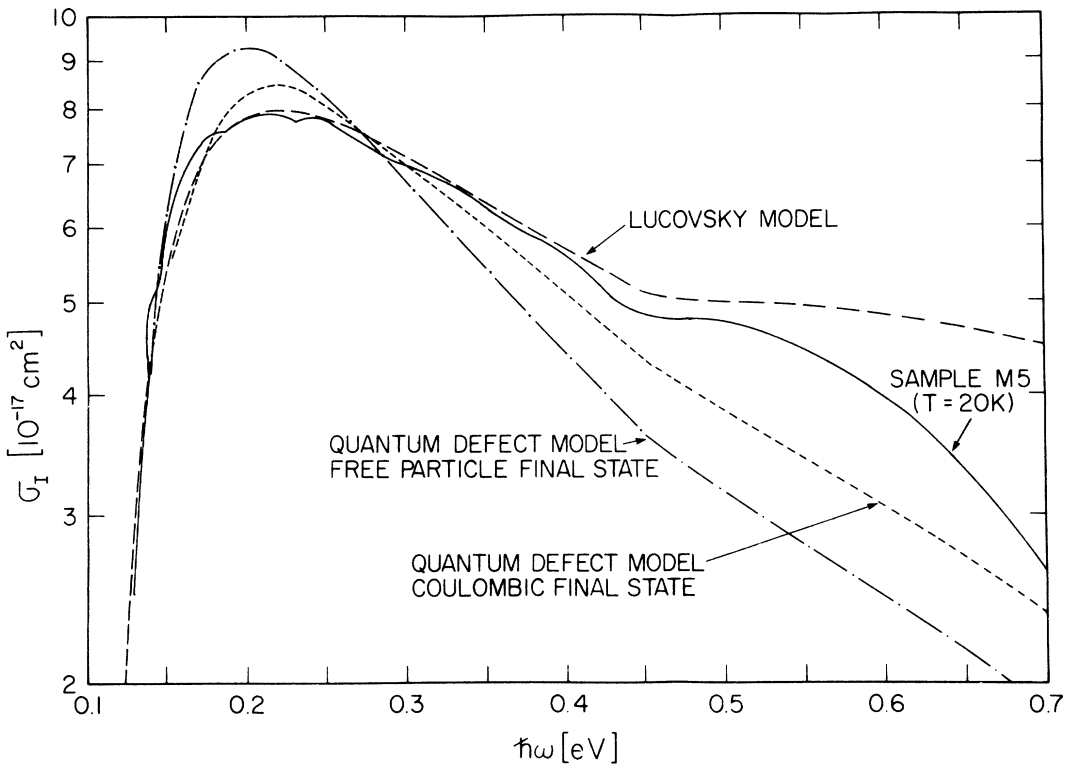

FIG. 3. Photoionization cross section vs photon energy for crystal $M5$ (20-K data) compared with three deep impurity models, each characterized by a choice of $E_a = 0.110$ eV. Lucovsky model (Ref. 8) is shown for $(\epsilon_{eff}/\epsilon_0) = 0.98$. Quantum-defect model with Coulomb final state is shown for $\nu = 0.52$, $\mu = -0.17$, and $(\epsilon_{eff}/\epsilon_0) = 1.4$. Quantum-defect model with free-wave final state (Ref. 10) is shown for $\nu = 0.52$ and $(\epsilon_{eff}/\epsilon_0) = 0.93$. The theoretical curves are shown augmented above 0.46 eV by photoionization contributions to the split-off band, as discussed in the text.

In Sec. III we shall comment on some theoretical models for deep impurities, and the photoionization curves to be expected from these models. Section IV will compare such models with the 20-K data shown for crystal $M5$ in Fig. 2. There are valid reasons for selecting this as the most reliable of our curves. We know from detailed transport measurements that the material of $M6$ and $M7$ has a less homogeneous manganese distribution than $M5$; moreover, $M5$ is much less heavily compensated. Since $M1$ is weakly doped, the optical density (αt) is little more than unity for this sample even at 0.2 eV, and becomes too small for precise evaluation at lower and higher photon energies. Nonetheless, it is reassuring that our four crystals all yield *approximately* the same maximum value for σ_I.

The models of Sec. III are discussed in terms of photoionization into the uppermost (light and heavy hole) valence bands, with a threshold at 0.11 eV. Optically, we also see photoionization into the split-off band above a threshold $E_a + \Delta = 0.46$ eV, which accounts for a change in slope at 0.46 eV in the various curves of Fig. 2. A weak absorption (visible in several of the 77-K curves of Fig. 2) occurs at 0.35 eV when optical transmission is measured with a few free holes present in the heavy hole band; these holes are then eligible for intraband transitions to the split-off band.[5] This intraband process is absent from the 20-K data of crystal $M5$.

III. DEEP IMPURITY MODELS

Lucovsky[8] has suggested a simplified model for a deep impurity in which the binding of the hole results from a short-range core potential rather than a graduated Coulomb potential. Intermediate between the Lucovsky model and that of a shallow hydrogenic impurity lie the quantum-defect models developed for semiconductor use by Bebb and Chapman.[9–11] It is of interest to compare our data with these models.

Choice of the parameters $N_0 = 3.33$ for the refractive index and $\kappa = 12.5$ for the dielectric constant of GaAs, together with $m_v = 0.34 m_0$ as the relevant heavy hole mass parameter,[9] tells us that a *shallow* acceptor in this solid should be characterized by a hydrogenic wave function with

$$a_H = (\hbar^2\kappa/m_v e^2) = 19.4 \text{ Å}\,,$$
$$E_H = (e^2/2\kappa a_H) = 0.030 \text{ eV}\,. \quad (5)$$

This is indeed just about the activation energy seen for shallow (zinc) acceptors.[12]

A parameter with the dimensions of area which enters into the description of photoionization for both hydrogenic and nonhydrogenic models is

$$A_a = (4\pi N_0 \kappa \hbar^3/3ce^2 m_v^2)\,. \quad (6)$$

For p-type GaAs, this has the value $A_a = 3.08\times10^{-16}$ cm^2. A hydrogenic impurity should exhibit a maximum photoionization cross section of $128\pi A_a/e^4 = 7.37A_a$ for $\hbar\omega \simeq E_H$, with the cross section falling off as $(\hbar\omega)^{-7/2}$ at high energies.[13] This falloff is a consequence of the rapidly attenuating density of bound states as one proceeds away from the origin of momentum space.

The increased localization of a bound hole on a deep impurity spreads the density of bound states further out in momentum space; thus regardless of the potential or wave-function characterization chosen for a deep impurity, we expect to see a photoionization cross section which is smaller than for a shallow center and which reaches its maximum value at a photon energy well above threshold.

The Lucovsky model neglects the Coulomb potential completely and approximates the strong ion-core potential by a δ function, with magnitude adjusted to give a characteristic length which corresponds with the observed ionization energy. As Lucovsky notes, the model corresponds with the deuteron binding model of nuclear physics, and enables us to use the deuteron result for photoionization of the cross section. With a δ-function potential, the ground state has a wave function

$$\psi(r) = (2\pi r^2 a_L)^{-1/2} e^{-r/a_L}\,, \quad (7)$$

where

$$a_L = a_H(E_H/E_a)^{1/2} = (\hbar^2/2m_v E_a)^{1/2}\,. \quad (8)$$

Since $E_a = 0.110$ eV for manganese acceptors in GaAs, $a_L = 10.1$ Å for the bound state. With the interaction of a photon field between this bound state and a free-plane-wave final state handled in the electric dipole approximation, σ_I is

$$\sigma_I = A_a(E_H/E_a)(\epsilon_{eff}/\epsilon_0)^2[8E_a^{3/2}(\hbar\omega - E_a)^{3/2}/(\hbar\omega)^3]$$
$$= \sigma_{max}[8E_a^{3/2}(\hbar\omega - E_a)^{3/2}/(\hbar\omega)^3]\,. \quad (9)$$

The quantity in square brackets in Eq. (9) reaches its maximum value of unity for $\hbar\omega = 2E_a$, as exemplified by the maximum at 0.22 eV for the Lucovsky curve in Fig. 3. The Lucovsky curve and the two other theoretical curves for the quantum-defect models show the additional contribution above 0.46 eV of photoionization into the split-off band. We shall return later to the topic of transitions into this lower band.

The maximum cross section of Eq. (9) varies as the square of the "effective-field ratio" $(\epsilon_{eff}/\epsilon_0)$. Dexter[14] has discussed the anticipated enhancement of the effective electric field of a photon in the immediate vicinity of a highly localized center embedded in a medium of high dielectric constant. Under conditions which make Dexter's arguments valid, $(\epsilon_{eff}/\epsilon_0)$ will exceed unity. However, the Lucovksy model curve of Fig. 3 is plotted for $A_a = 3.08\times10^{-16}$ cm^2, $E_H = 0.030$ eV, $E_a = 0.110$ eV, and $(\epsilon_{eff}/\epsilon_0) = 0.98$, to make $\sigma_{max} = 8.0\times10^{-17}$ cm^2.

The Lucovsky δ-function-potential model is an extreme example of supposing a highly localized non-Coulomb potential—thus this model predicts no excited states at all. (The shallow excited states seen in practice must be invoked from the Coulomb wings outside the core potential.) The consequences for photoionization are less drastic than might be supposed, and Lucovsky notes that the calculation of σ_I is rather insensitive to the exact form chosen for the short range potential.

Intermediate between Eq. (7) and a scaled hydrogenic $1s$ wave function lies the quantum-defect wave function adapted by Bebb and Chapman[9-11] for use in semiconductor photoionization problems. The technique may be applied any time that an asymptotic wave function is known along with the activation energy, while the behavior within some core is not known. The wave function outside the core may be assumed to be a solution to the Coulomb tail. Furthermore, this need not be well-behaved inside the core, though it must be continuous with the true core solution. First a (nonintegral) effective quantum number ν is obtained for the ground state in terms of E_a and the hydrogenic energy E_H:

$$\nu = (E_H/E_a)^{1/2}\,. \quad (10)$$

The amount by which ν is depressed below unity is the "quantum defect." The large-radius asymptotic form of the bound-state wave function is

$$\psi(r) = \frac{(2r/\nu a_H)^\nu}{[2\pi\nu a_H r^2\Gamma(2\nu+1)]^{1/2}}\, e^{-r/\nu a_H}\,, \quad (11)$$

and it is worth noting from Eqs. (8) and (10) that the characteristic length νa_H in Eq. (11) is identical with the quantity a_L of the Lucovsky model [which Eq. (11) approaches as $\nu \to 0$].

Bebb and Chapman initially[9] calulated σ_I from the bound state of Eq. (11) to a Coulomb continuum final state,[15] and this approach yielded families of graphical results. Since the continuum states were adjusted separately with an estimated "continuum quantum defect" $\mu(k^2)$, both ν and μ must be specified as characterizing the spectral shape factor $F(\hbar\omega)_{\nu,\mu}$ for the photoionization cross section

$$\sigma_I = \sigma_{max} F(\hbar\omega)_{\nu,\mu}\,. \quad (12)$$

The values of ν and μ, as well as A_a and $(\epsilon_{eff}/\epsilon_0)$, also determine σ_{max}. Figure 3 shows one curve for the Coulomb continuum version of the quantum-defect model, with parameters chosen to be suitable for a comparison with manganese: $E_a = 0.110$ eV (so that $\nu = 0.52$ and $\nu a_H = 10.1$ Å) $\mu = -0.17$, $A_a = 3.08 \times 10^{-16}$ cm^2, and $(\epsilon_{eff}/\epsilon_0) = 1.4$. The values decided upon for ν and μ are very close to those suggested by Bebb and Chapman[9] as relevant for manganese in GaAs, and the spectral location of the maximum is quite sensitive to the choice for ν.

Bebb[10] subsequently recalculated σ_I using Eq. (11) for the bound state and a free wave final state; this yields σ_I as an analytic function of photon energy parametrized by ν. Figure 3 shows the curve which results for $E_a = 0.110$ eV and $\nu = 0.52$. This particular value of ν results in a maximum cross section

$$\sigma_{max} = 0.35 A_a (\epsilon_{eff}/\epsilon_0)^2 \tag{13}$$

and a value $(\epsilon_{eff}/\epsilon_0) = 0.93$ is chosen to set the maximum of the curve in Fig. 3. This curve above 0.46 eV shows the added contribution calculated for the companion process of photoionization into the split-off band, also using $\epsilon_{eff}/\epsilon_0 = 0.93$. The contribution of this latter process reaches a maximum between 0.6 and 0.7 eV.

The Bebb quantum-defect model with a Coulombic final state is not in a form which is amenable to calculation of the strength of transitions to the split-off band. As an estimate of the effect of such transitions on the "Coulombic final-state" curve of Fig. 3, we have simply added a contribution equal to that calculated for the "free-particle final-state" model, except for the assumption of a unity effective-field ratio.

IV. DISCUSSION AND CONCLUSIONS

In conformity with the known activation energy for Mn acceptors, the value $E_a = 0.11$ eV was used in calculating the three theoretical curves of Fig. 3 up to 0.46 eV. (The abovementioned process of transitions to the split-off band affected the shapes of the curves above 0.46 eV.) For the Lucovsky model, the only other disposable parameter is $(\epsilon_{eff}/\epsilon_0)$. This can be used to scale the maximum, but does not affect the shape of the curve. Thus we consider the Lucovsky model to give a successful fit to the data of our crystal $M5$ over the range 0.12–0.4 eV, with a maximum at the observed energy, and a magnitude of cross section which fits the observed data for an effective-field ratio negligibly different from unity.

Since $E_H = 0.030$ eV in p-type GaAs, the principal quantum number has to be $\nu = 0.52$ for quantum-defect models. The effective-field ratio is once more the only adjustable parameter for the plane-wave final-state version of this model. Additional flexibility in curve fitting is provided in the Coulomb continuum version of the quantum-defect model through the defect number μ.

For either version of the quantum-defect model, the value of $(\epsilon_{eff}/\epsilon_0)$ necessary to make the computed σ_{max} approximate the measured σ_{max} is not far from unity. However, the free-particle final-state version of this model achieves its maximum at an energy appreciably less than we find experimentally, and the rate at which σ_I decreases from 0.25 to 0.45 eV is steeper than found for any of our samples (with the possible exception of the less than ideal data for crystal $M1$).

Thus the Lucovsky model appears to give a better prediction of the course of σ_I up to 0.46 eV. However, the δ-function potential approach predicts a photoionization contribution to the split-off band which has its maximum effect at 0.9 eV, and which (with the continued assumption of a unity effective-field ratio) seems considerably larger than seen experimentally.

The added absorption seen above 0.46 eV for crystal $M5$ that we can attribute to transitions down to the split-off band thus appears to be smaller than expected for a bound-state wave function described by Eq. (7), yet possibly larger than expected for the wave function of Eq. (11). In this respect, examination of the transitions to the split-off band probably gives one a more sensitive test for the form of ψ than examination of the region above the first 0.11-eV threshold, since the states of small wave vector are scrutinized over a larger energy range. σ_I, and the agreement between experiment and this model, in Fig. 3 is quite satisfactory.

Another very satisfactory conclusion from Fig. 3 is that the value of $(\epsilon_{eff}/\epsilon_0)$ required to make any deep impurity model fit the data for manganese is close to unity. Dielectric enhancement of a photon's electric vector just does not happen to an appreciable extent with this impurity. This is not surprising when we note that the various models predict ground-state wave functions with a characteristic length $a_L = \nu a_H = 10.1$Å. Since this is more than four times larger than the nearest-neighbor distance in GaAs, manganese is not a truly compact localized center in the tight-binding sense. The charge distribution corresponding to the wave function of Eq. (7) places a charge of $0.79e$ outside a sphere with the 2.45-Å nearest-neighbor distance as diameter, while $0.62e$ lies outside a sphere of *radius* 2.45 Å. Thus the bound hole moves most of the time through regions of space for which the macroscopic dielectric constant is a valid concept.

ACKNOWLEDGMENTS

We wish to acknowledge the sponsorship of this research by the U. S. Air Force Office of Scientific

Research, under Grant AFOSR-72-2175. Thanks are due to Dr. G. R. Cronin and Dr. R. A. Chapman for several of the crystals we have measured. We are indebted to Merrill Stass for her help with these measurements, and to Douglas Cohen for his assistance in developing the high-temperature-measurement technique. We also wish to thank Professor H. J. Queisser, Dr. H. B. Bebb, and Dr. R. A. Chapman for helpful discussions and communication of unpublished results.

---

*Research supported in part by the U. S. Air Force Office of Scientific Research, under Grant No. AFOSR-72-2175.

†Present address: Research Flight Facility, N.O.A.A., Miami, Fla.

[1]L. J. Vieland, J. Appl. Phys. **33**, 2007 (1962).

[2]R. W. Haisty and G. R. Cronin, in *Proceedings of the Seventh International Conference on the Physics of Semiconductors, Paris, 1964* (Academic, New York, 1965), p. 1161.

[3]R. A. Chapman and W. G. Hutchinson, Phys. Rev. Lett. **18**, 443 (1967).

[4]See, for example, T. C. Lee and W. W. Anderson, Solid State Commun. **2**, 265 (1964).

[5]W. J. Brown, Jr. and J. S. Blakemore, J. Appl. Phys. **43**, 2242 (1972).

[6]M. Blätte, dissertation (University of Frankfurt, 1970) (unpublished); data incorporated in paper by H. J. Queisser [in *Festkörperprobleme XI,* edited by O. Madelung (Pergamon, Vieweg, 1971), p. 45].

[7]J. S. Blakemore, W. J. Brown, M. L. Stass, and D. A. Woodbury, J. Appl. Phys. 44, 3352 (1973).

[8]G. Lucovsky, Solid State Commun. **3**, 299 (1965).

[9]H. B. Bebb and R. A. Chapman, J. Phys. Chem. Solids **28**, 2087 (1967).

[10]H. B. Bebb, Phys. Rev. **185**, 1116 (1969).

[11]H. B. Bebb and R. A. Chapman, in *Proceedings of the Third International Photoconductivity Conference, Stanford, 1969* (Pergamon, Oxford, England, 1971), p. 245.

[12]D. E. Hill, J. Appl. Phys. **41**, 1815 (1970).

[13]M. Lax, *Photoconductivity Conference, 1954* (Wiley, New York, 1956), p. 111.

[14]D. L. Dexter, in *Solid State Physics*, edited by F. Seitz *et al.* (Academic, New York, 1958), Vol. 6, p. 353.

[15]A. Messiah, *Quantum Mechanics* (Wiley, New York, 1959).